

Simplexviruses successfully adapt to their host by fine-tuning immune responses

Alessandra Mozzi^{1*}\$, Rachele Cagliani^{1*}, Chiara Pontremoli¹, Diego Forni¹, Irma Saulle^{2,3}, Marina Saresella⁴, Uberto Pozzoli¹, Mario Clerici^{3,4}, Mara Biasin², Manuela Sironi¹

* equal contribution

\$ corresponding author

¹ Scientific Institute, IRCCS E. MEDEA, Bioinformatics, 23842 Bosisio Parini, Italy.

² Department of Biomedical and Clinical Sciences "L. Sacco", University of Milan, 20157 Milan, Italy.

³ Department of Physiopathology and Transplantation, University of Milan, 20090 Milan, Italy.

⁴ Don C. Gnocchi Foundation ONLUS, IRCCS, Laboratory of Molecular Medicine and Biotechnology, 20148, Milan, Italy.

Corresponding author: Alessandra Mozzi, Bioinformatics - Scientific Institute IRCCS E. MEDEA, 23842 Bosisio Parini, Italy. e-mail: alessandra.mozzi@lanostrafamiglia.it

1 **Abstract**

2

3 Primate herpes simplex viruses are relatively harmless to their natural hosts, whereas cross-species
4 transmission can result in severe disease. We performed a genome-wide scan for signals of
5 adaptation of simplexviruses to hominins. We found evidence of positive selection in three
6 glycoproteins, with selected sites located in antigenic determinants. Positively selected non-core
7 proteins were involved in different immune-escape mechanisms. By expressing mutants of one of
8 these proteins (ICP47), we show that the amino acid status at the positively selected sites is
9 sufficient to induce HLA-G. HSV-1/HSV-2 ICP47 induced HLA-G when mutated to recapitulate
10 residues in B virus, whereas the mutated version of B virus ICP47 failed to determine HLA-G
11 expression. Thus, the evolution of ICP47 in HSV-1/HSV-2 determined the loss of an
12 immunosuppressive effect, suggesting that simplexviruses tune immune responses to promote
13 successful co-existence with their hosts. These results also help explain the high pathogenicity of B
14 virus in humans.

15 **Introduction**

16

17 Herpes simplex viruses (genus *Simplexvirus*, family *Herpesviridae*, order *Herpesvirales*), are dsDNA
18 viruses that infect mammals, including humans and other primates. They have long genomes of
19 approximately 155 kbp, organized into two regions of unique sequence (long (UL) and short (US))
20 flanked by direct or inverted repeats. The two unique sequences contain the great majority of the
21 protein-coding regions, including core genes, which are shared among herpesviruses, and non-core
22 genes, that are specific for members of the *Alphaherpesvirinae* subfamily and/or of the
23 *Simplexvirus* genus only (McGeoch et al., 2006).

24 In analogy to other herpesviruses, the evolutionary history of simplexviruses was mainly
25 characterized by coevolution and codivergence with their hosts (McGeoch et al., 2006). A known
26 exception is represented by human herpes simplex virus 2 (HSV-2), which most likely originated
27 from the cross-species transmission of an ancestor of chimpanzee herpesvirus 1 (PanHV-3) to an
28 ancestor of modern humans, around 1.6 million years ago (Severini et al., 2013; Underdown et al.,
29 2017; Wertheim et al., 2014). Thus, whereas most primates are infected by a single simplexvirus,
30 humans host two: HSV-2 and human herpes simplex virus 1 (HSV-1). These viruses are present at
31 high prevalence in human populations. Estimates vary with geography and reach 67% (HSV-1) and
32 11% (HSV-2) of the world population (Looker et al., 2015a; Looker et al., 2015b). Even if HSV-1 is
33 primarily responsible for oro-facial lesions and HSV-2 for genital herpes (Arvin et al., 2007), both
34 viruses can establish latency in trigeminal and lumbosacral ganglia, resulting in life-long infection
35 (Arvin et al., 2007). Whereas a relatively low proportion of infected individuals show clinical
36 manifestations during primary infection or reactivation (Tognarelli et al., 2019), simplexviruses can
37 occasionally determine severe diseases such as infectious blindness, acute encephalitis, and
38 neonatal invasive infection (Farooq and Shukla, 2012; Whitley, 2004).

39 In non-human primates (NHP), simplexvirus infections show symptoms and seroprevalence
40 generally comparable to those of HSV-1 and HSV-2, and these viruses are species-specific in natural
41 settings (Eberle and Jones-Engel, 2017). This feature, together with the near commensal
42 relationship with their hosts, is in line with long-standing virus-host coevolution. Indeed, the
43 consequences arising from disruption of the delicate balance established during millions of years of
44 coexistence are evident when cross-species transmissions occur. For instance, macacine
45 herpesvirus 1 (McHV1, also known as B virus) is almost asymptomatic in macaques, but infection of
46 humans or African monkeys results in a severe, often fatal form of encephalomyelitis (Eberle and
47 Jones-Engel, 2017; Loomis et al., 1981; Tischer and Osterrieder, 2010; Wilson et al., 1990).

48 Likewise, the transmission of HSV-1 from humans to marmosets or other New World monkeys is
49 almost invariably fatal (Azab et al., 2018; Tischer and Osterrieder, 2010). These examples clearly
50 testify how the viral and host genomes interact to determine the outcome of infection and
51 highlight the potential zoonotic threat posed by simplexviruses. This also implies that
52 simplexviruses must have adapted to their hosts and that the signatures of such adaptation may be
53 detected using molecular evolution approaches. We thus performed a genome-wide scan of
54 positive selection to identify variants in simplexvirus coding genes that arose during adaptation to
55 the hominin lineage. As a proof of concept, we tested the functional effect of selected variants in
56 *US12*, which encodes the ICP47 TAP inhibitor, a modulator of immune response.

57

58 **Results**

59

60 **Selective patterns of catarrhini-infecting simplexvirus coding genes**

61 We first explored the selective patterns of primate simplexvirus coding genes. We thus analyzed 6
62 complete genomes of simplexviruses that infect different primates, from hominins (HSV-1, HSV-2,
63 and ChHV) to Old World African and Asian monkeys (CeHV-2, PaHV-2, and McHV-1) (Figure 1A,
64 Table S1).

65 Because high sequence diversity can affect evolutionary inference, viruses that infect New World
66 primates were excluded from these analyses. Analysis of selective patterns was performed for all
67 coding genes with reliable one-to-one orthologs. Gene sequences were rigorously filtered to
68 ensure high quality alignments (see Materials and Methods). Genes for which few orthologous
69 sequences were retrieved or with extended overlapping ORFs, were discarded (Table S2). The
70 average non-synonymous substitution/synonymous substitution rate (dN/dS, also referred to as ω)
71 was calculated for the resulting 65 genes (Table S3). Comparison of ω values among *core* genes
72 (conserved among *Herpesviridae*, n=38) and *non-core* genes (specific to simplexviruses, n=27)
73 indicated that these latter show lower evolutionary constraint (Wilcoxon Rank Sum test, p= 0.011)
74 (Figure 1B, Table S3).

75

76 **Adaptive evolution in the hominin-infecting simplexvirus lineage**

77 In order to assess whether adaptation to hominins drove the evolution of specific simplexvirus
78 coding genes, we applied a branch-site test (Zhang et al., 2005) to an extended phylogeny of 53
79 viruses that infect hominins, Old World African monkeys, and Old world Asian monkeys (Figure 1A,
80 Table S1). In the branch-site test, the branches of the tree are divided *a priori* into foreground and

81 background lineages, and models that allow or disallow positive selection on the foreground
82 lineage(s) are compared. The branch-site test can thus detect lineage-specific selected genes and
83 sites (episodic positive selection). Herein, we set the branch leading to the hominin-infecting
84 simplexviruses as foreground (Figure 1A).

85 After accounting for recombination (see Materials and Methods), we found evidence of adaptive
86 evolution for 11 genes (16.9%). Positive selection in hominin simplexviruses similarly targeted *core*
87 and *non-core* genes (selected fraction = 15.8% and 18.5%), irrespective of the higher selective
88 constraint observed in *core* genes during viral evolution in catarrhini (Table S4).

89 We next analyzed positively selected sites. To be conservative, these were detected by the
90 intersection of two approaches (see Materials and Methods). Among the *core* genes, we found
91 evidence of episodic positive selection for three glycoproteins: gB (UL27), gH (UL22) and gM (UL10)
92 (Figure 2 and Figure S1). *UL27* encodes the viral envelope glycoprotein B (gB), which is a major
93 target antigen in herpesviruses (Malito et al., 2018). Both selected sites in gB are located in the
94 ectodomain (Figure 2) and one of them, A334, is part of an epitope recognized by the SS55
95 neutralizing antibody (Cairns et al., 2014) (Figure 2). Interestingly, an R-to-Q substitution at residue
96 335, confers resistance to the SS55 mAb (Cairns et al., 2014). As for gH, two positively selected
97 sites, Y85 and E170, flanked amino acids that, if mutagenized, confer resistance to the potent LP11
98 neutralizing antibody (Figure 2) (Chowdary et al., 2010). Because the LP11 antibody competes with
99 gB for binding to the gH-gL complex, the gB binding site was proposed to be in close proximity to
100 (or maybe overlapping) with the LP11 epitope surface (Chowdary et al., 2010). E170 is part of this
101 surface, together with other sites we found under positive selection (Figure 2). Overall, these
102 observations suggest that the selective pressure acting on these two glycoproteins is exerted by
103 the host immune system.

104 We also found many positively selected sites in gM (UL10); the N-terminus of gM is predicted to
105 interact with the glycoprotein N (gN), to form a stable complex, which modulates the viral fusion
106 machinery (El Kasmi and Lippé, 2015). Three of the positively selected sites (S51, R56, P58) we
107 found, are located in the surface exposed region of gM, just upstream the cystein (C59) residue
108 which is responsible for an interchain disulphide bond that stabilize the gM-gN complex
109 (Striebinger et al., 2016), strongly suggesting that these residues could contribute to gM-gN
110 interaction. Several other positively selected sites were located along the whole sequence of gM
111 (Figure 2).

112 Among *non-core* genes showing evidence of positive selection, four (*UL46*, *US8*, *US1*, and *US12*)
113 are involved in different immune-escape mechanisms. *US8* codes for glycoprotein E (gE) that, in

114 complex with gI, forms an Fc receptor for immunoglobulin G (IgG) (Dubin et al., 1991; Sprague et
115 al., 2006). The gE-gI complex binds the Fc region of IgG leading to an antibody bipolar bridging on
116 infected cells, preventing IgG-mediated immune response. In US8, six positively selected sites were
117 found in the protein domain involved in Fc interaction; among them, E227 and G313 lies at Fc
118 interaction surface boundaries (Figure 3) (Sprague et al., 2006).

119 UL46 encodes an abundant tegument protein that mediates viral evasion from foreign DNA-sensing
120 pathways (Deschamps and Kalamvoki, 2017). In particular, the UL46 protein of HSV-1 interacts with
121 both TMEM173/STING and TBK1 through separate domains and blocks the DNA-sensing pathway.
122 We detected positively selected sites both in the STING and in the TBK1 binding regions (Figure 3).

123 US1 encodes the ICP22 protein (Figure 3), a general transcription regulator that also down-
124 modulates the expression of CD80 in dendritic cells (Matundan and Ghiasi, 2019). Finally, US12
125 encodes the ICP47 protein, which down-regulates the expression of major histocompatibility
126 complex (MHC) class I molecules on the cell surface (Früh et al., 1995; Hill et al., 1995). In
127 particular, the ICP47 proteins of HSV-1 and HSV-2 act as inhibitors of the transporter associated
128 with antigen processing (TAP), which translocates antigenic peptides into the endoplasmic
129 reticulum lumen for loading onto MHC class I (HLA-ABC) molecules (Früh et al., 1995; Hill et al.,
130 1995; Tomazin et al., 1998). The TAP-biding region resides in the N-terminal portion of the ICP47
131 protein, where all the positively selected sites are located (Galocha et al., 1997; Matschulla et al.,
132 2017) (Figures 3 and 4A-B).

133

134 **Positively selected sites in *US12* modulate the surface expression of MHC class I molecules.**

135 The N-terminal region of ICP47 is poorly conserved across hominin-infecting SVs, and considerable
136 divergence is also observed between HSV-1 and HSV-2, which however bind and inhibit human TAP
137 (Tomazin et al., 1998). In particular, the 55 N-terminal residues of HSV-1 ICP47 are sufficient to
138 interact with and inhibit TAP (Galocha et al., 1997; Matschulla et al., 2017). Conversely, a previous
139 study indicated that the ICP47 protein encoded by B virus lacks the ability of HLA-ABC down-
140 regulation, although up-regulation of HLA-E and HLA-G was observed during infection (Vasireddi
141 and Hilliard, 2012). We thus investigated whether the positively selected sites in ICP47 modulate
142 the different ability of simplexvirus proteins to regulate HLA-ABC expression, and if the ICP47
143 protein of B virus is responsible for HLA-G up-regulation. To this aim, we designed constructs
144 carrying the TAP binding domains of HSV-1, HSV-2, or the corresponding region of B virus ICP47.
145 Two additional constructs carried the HSV-1 or HSV-2 ICP47 N-terminal domain mutagenized at the
146 positively selected sites to recapitulate the amino acid state observed in the macaque virus. In

147 turn, mutations reproducing the amino acids observed in the human virus were introduced in the B
148 virus N-terminal domain (Figure 4B).

149 These constructs, together with a plasmid expressing the full-length HSV-1 ICP47 protein, were
150 transiently transfected in Jurkat cells and the surface expression of HLA-ABC molecules was
151 evaluated by cytofluorimetry. As expected, a significant effect of the plasmids on HLA-ABC
152 expression was evident (ANOVA, $F = 19.55$, $P = 7.22 \times 10^{-8}$), whereas the differences among
153 replicates were not significant ($F = 2.57$, $P = 0.08$). Tukey post hoc tests indicated that the full-
154 length ICP47 protein and the two TAP binding domains of HSV-1 and HSV-2 significantly reduced
155 HLA-ABC expression compared to mock transfected cells (Figure 4C). No difference was observed
156 between the two short constructs and the complete ICP47 protein. Mutation of the positively
157 selected sites in both the HSV-1 and HSV-2 TAP biding domains of ICP47 totally abolished these
158 effects (Figure 4C), suggesting that the selected sites play an important role in TAP binding. In line
159 with previous results (Vasireddi and Hilliard, 2012), the ICP47 domain of B virus did not affect HLA-
160 ABC expression, However, mutation of the selected sites to recapitulate the amino acids observed
161 in the HSV-1/HSV-2 molecules was not sufficient to restore TAP inhibition (Figure 4C). Overall, these
162 results indicate that the positively selected sites are not the sole determinants of TAP binding.

163 We next assessed the effect of the different ICP47 constructs on HLA-G expression. Again, a
164 significant effect for the constructs (ANOVA, $F = 53.28$, $P = 5.91 \times 10^{-12}$) but not for the replicates (F
165 $= 0.73$, $P = 0.55$) was observed. The short N-terminal domain of B virus ICP47 was sufficient to
166 significantly increase HLA-G expression compared to mock-transfected cells (Figure 4D). Mutation
167 of the positively selected sites to those observed in HSV-1 and HSV-2 fully abrogated the increased
168 expression of HLA-G. Interestingly, whereas the expression of full or partial HSV-1/HSV-2 ICP47 did
169 not affect HLA-G expression, introduction of mutations that recapitulate amino acids observed in B
170 virus conferred to both ICP47 N-terminal domains the ability to induce HLA-G (Figure 4D). These
171 results indicate that the modulatory effect of B virus on HLA-G expression is mediated by the N-
172 terminal domain of ICP47 and that the positively selected sites are the major determinants of HLA-
173 G regulation. Clearly, the effect on HLA-G expression must be TAP-independent.

174

175 **Discussion**

176

177 Primate simplexviruses are often regarded as an epitome of virus-host coevolution and
178 codivergence (Eberle and Jones-Engel, 2017; McGeoch et al., 2006). These viruses establish life-
179 long infections and usually cause little harm to their hosts, whereas periodic viral reactivation

180 allows transmission in the population. Indeed, virulence and host range are often interconnected
181 traits in viruses (Rothenburg and Brennan, 2020), which are expected to evolve to maximize their
182 transmission potential in the host and to tune their virulence accordingly.
183 Whereas several herpesviruses are unable to infect species other than their natural host, the
184 occasional cross-species transmission of primate simplexviruses has been documented several
185 times, indicating that few barriers exist in terms of infection potential (Azab et al., 2018). However,
186 most spill-overs result in a very severe disease in the new host, especially when the phylogenetic
187 distance from the original host is considerable (Azab et al., 2018). For instance, HSV-1 infection is
188 almost invariably fatal in New World monkeys, whereas limited data on gorillas and Old World
189 monkeys suggest that the symptoms are milder (Gilardi et al., 2014; Tischer and Osterrieder, 2010).
190 The best known example of the severe effects of cross-species transmission is that of B virus.
191 Although the virus is rarely acquired, even in people who are in frequent contact with macaques,
192 mortality due to central nervous system involvement is extremely high when infection occurs (Azab
193 et al., 2018; Eberle and Jones-Engel, 2018; Tischer and Osterrieder, 2010).
194 These observations clearly indicate that simplexviruses have been adapting to their hosts to
195 balance virulence and transmission. Such a balance is most likely the result of multiple interactions
196 between virus- and host-encoded factors, and the interplay between the host immune response
197 and the viral evasion strategies is expected to determine the outcome of infection. We thus
198 searched for signals of adaptation of simplexviruses to their hominin hosts. Specifically, we applied
199 a branch-site test, which is well-suited to identify episodic positive selection - i.e., selection events
200 that occurred on a specific branch of a phylogeny. Among *core* genes, we found evidence of
201 episodic positive selection in three glycoproteins, namely gB, gM, and gH, all of which contribute
202 to virus cell entry via membrane fusion (Arii and Kawaguchi, 2018; El Kasmi and Lippé, 2015). For
203 gB and gH we found that some of the positively selected sites map to antigenic determinants,
204 suggesting that the host adaptive immune response represents the underlying selective pressure.
205 Moreover, these glycoproteins participate in other processes that contribute to the alteration of
206 the host immune responses. In fact, gB affects the trafficking of MHC class II molecules and diverts
207 them to the exosome pathway (Temme et al., 2010), whereas gH interacts with both $\alpha\beta 3$ -integrin
208 and TLR2, which sense the virus and activate the innate immune response (Gianni et al., 2012;
209 Leoni et al., 2012). Both gH and gM were also reported to counteract tetherin, a cellular restriction
210 factor for several enveloped viruses (Blondeau et al., 2013; Liu et al., 2015). In line with the view
211 that hosts and viruses are engaged in genetic conflicts, tetherin was shown to have evolved under
212 positive selection in primates (Gupta et al., 2009; Lim et al., 2010; McNatt et al., 2009). Indeed, this

213 is a general finding for a number of genes involved in defense mechanisms, which display unusually
214 rapid rates of evolution in response to the selective pressure imposed by pathogens (Sironi et al.,
215 2015). Clearly, several infectious agents can insist on the same defense pathway, implying that
216 pathogens are faced with a fast-evolving array of host defense mechanisms. For instance, STING, a
217 stimulator of interferon responsive genes, which is positively selected in primates (Mozzi et al.,
218 2015), is targeted by several viruses. We found three positively selected sites in the STING-binding
219 domain of UL46, suggesting virus adaptation to modulate interaction with the host molecule.
220 Another cellular system commonly antagonized by viruses is the antigen processing and
221 presentation pathway, many components of which show rapid evolutionary rates (Forni et al.,
222 2014). In particular, different herpesviruses employ distinct strategies to interfere with the antigen
223 presentation pathway, thus protecting themselves from the host immune response (van de Weijer
224 et al., 2015; Verweij et al., 2015). In addition to the above-mentioned effect of gB on MHC class II
225 sorting, simplexviruses express the ICP22 protein, which is positively selected and down-modulates
226 CD80 (Matundan and Ghiasi, 2019), as well as the ICP34.5 protein (the product of *RL1*). ICP34.5, a
227 neurovirulence factor that blocks MHC II expression on the surface of infected cells (Trgovcich et
228 al., 2002). Due to the small number of confirmed orthologs of *RL1* we could no test whether
229 positive selection acted on this gene.
230 We instead analyzed the selection pattern of *US12*, which encodes ICP47. All but one of the
231 positively selected sites we detected were located within the N-terminal domain. For the HSV-1
232 ICP47 protein, this region is sufficient to bind TAP and freeze it in an inactive conformation
233 (Galocha et al., 1997; Matschulla et al., 2017). Because peptide loading is necessary to allow
234 folding of HLA class I molecules in their active configuration, this in turn results in the retention of
235 HLA-ABC molecules in the endoplasmic reticulum. HLA-ABC down-regulation prevents the
236 recognition of infected cells by CD8⁺ T-lymphocytes, which explains why TAP inhibition is a
237 common viral strategy of immune subversion (Hill et al., 1995). The TAP binding activity of ICP47
238 was demonstrated for both the HSV-1 and HSV-2 proteins, although sequence similarity is limited
239 in the N-terminal portion. Conversely, infection with B virus does not result in the down-
240 modulation of HLA-ABC expression (Vasireddi and Hilliard, 2012). We thus reasoned that the
241 selected sites might underlie the different ability of simplex viruses to inhibit TAP. However, our
242 data indicate that, although the amino acid status at these sites is clearly important, as their
243 mutation in HSV-1/HSV-2 ICP47 restored HLA-ABC expression to the same level as non-transfected
244 cells, they do not represent the sole determinants of TAP binding. In fact, when the amino acids
245 observed in the human viruses were introduced in the N-terminus of B virus ICP47, no HLA-ABC

246 down-modulation was observed. Conversely, the amino acid status at the positively selected sites
247 is sufficient to determine HLA-G up-regulation. In fact, the N-terminal domains of both HSV-1 and
248 HSV-2 ICP47 induced HLA-G when mutated to recapitulate residues in B virus. Conversely, the
249 mutated version of B virus ICP47 failed to determine HLA-G expression. Overall, these results imply
250 that the ability of B virus to induce HLA-G resides in the N-terminal domain of ICP47 and that it
251 does not depend on TAP. This is consistent with the notion that HLA-G can be loaded with peptides
252 by both TAP-dependent and TAP-independent pathways (Lee et al., 1995). The mechanism
253 underlying the up-regulation of HLA-G by B virus ICP47 remains unexplored, and further
254 experiments will thus be required to determine how the positively selected sites exert their effect.
255 As a corollary, our data indicate that the short region of ICP47 we analyzed herein could be used as
256 an inducer of HLA-G expression, which is regarded as a potential biotherapy in allogenic
257 transplantation (Deschaseaux et al., 2011).

258 The reason why related viruses use the same protein to differentially modulate host responses
259 remains to be clarified. The loss of TAP-binding activity by B virus ICP47 may represent a strategy to
260 limit NK cell activation (Vasireddi and Hilliard, 2012). In fact, reduced HLA-ABC expression on the
261 cell surface results in NK-mediated killing, unless inhibitory ligands are also expressed (Früh et al.,
262 1995; Hill et al., 1995; Huard and Früh, 2000). Indeed, NK cells play a central role in limiting HSV-
263 1/HSV-2 infection, as demonstrated by mouse models (Rager-Zisman et al., 1987), as well as by the
264 extremely severe infection outcome in humans with genetic defects resulting in low/absent NK cell
265 counts (Orange, 2013). It was instead suggested that B virus, due to its lack of TAP-inhibitory
266 activity, does not trigger NK responses (Vasireddi and Hilliard, 2012). In addition, at least in human
267 cells, this virus up-regulates HLA-G (Vasireddi and Hilliard, 2012), which is associated with diverse
268 immunosuppressive functions, including inhibition of T cell and NK cell responses (Morandi et al.,
269 2016). On one hand these observations might account for the extreme virulence of B virus in
270 humans. On the other, as noted elsewhere (Eberle and Jones-Engel, 2018), they do not explain why
271 infection in macaques is poorly pathogenic. Notably, though, rhesus macaques do not express the
272 ortholog of HLA-G, as it is a pseudogene (Boyson et al., 1997). Through alternative splicing, the
273 Mamu-AG gene of these non-human primates encodes glycoproteins functionally similar to HLA-G
274 (Slukvin et al., 2000), which is also alternatively spliced. Mamu-AG shares several features with
275 human HLA-G, including a role in the establishment of maternal-fetal immune tolerance, but it is
276 phylogenetically more similar to HLA-A (Boyson et al., 1997). It is thus possible that Mamu-AG
277 glycoproteins are not up-regulated by ICP47 and that, therefore, infection in macaques elicits
278 weaker immunomodulatory effects, eventually resulting in mild presentation. Addressing this point

279 will require further analyses and the generation of antibodies against Mamu-AG, which are not
280 commercially available.

281 In summary, we performed a genome-wide scan of positive selection on the hominin simplexvirus
282 branch. We detected several positively selected sites, many of which most likely evolved in
283 response to immune-mediated selective pressure. As these sites were positively selected, they are
284 expected to affect some viral traits, as phenotypes are the ultimate target of selection. As a proof
285 of concept, we tested the functional effects of positively selected sites in ICP47. Such sites were
286 found to be sufficient to determine the inability of the viral protein to up-regulate HLA-G
287 expression. Thus, the evolution of ICP47 in HSV-1/HSV-2 determined the loss of an
288 immunosuppressive effect, suggesting that the trait under selection was decreased virulence. This
289 possibility parallels findings in human cytomegalovirus, another herpesvirus, whereby different
290 mechanisms promoting viral temperance were described (Dunn et al., 2003; Mozzi et al., 2020).
291 These analyses may also suggest that closely related viruses finely tune the balance between
292 immunosuppressive and immunostimulatory pathways to promote successful co-existence with
293 their primate hosts.

294

295 **Materials and Methods**

296

297 **Sequences and alignments**

298 Viral genome sequences were retrieved from the NCBI (<http://www.ncbi.nlm.nih.gov/>) database. A
299 detailed list of accession number is reported in Table S1. Alignments of whole genome sequences
300 were performed with Progressive MAUVE 2.3.1, using default parameters (Darling et al., 2004;
301 Darling et al., 2010). For each viral genome, we retrieved coding sequences of all annotated ORFs.
302 Orthology was inferred according to MAUVE attribution and to genome annotation.
303 Gene alignments were generated using MAFFT (Katoh and Standley, 2013), setting sequence type
304 as codons. Unreliably aligned codons were filtered using GUIDANCE2 (Sela et al., 2015) with a
305 cutoff of 0.90 (Privman et al., 2012). The resulting alignments were manually inspected.
306 Only reliable one-to-one orthologs were included in the subsequent analyses (Table S3).

307

308 **Selective patterns in primate-infecting simplexviruses**

309 The average dN/dS parameter was calculated using the single-likelihood ancestor counting (SLAC)
310 method (Kosakovsky Pond and Frost, 2005), using a phylogeny of 6 SVs infecting different primate
311 species (Table S1) .

312 Phylogenetic trees were generated with the phyML program (version 3.1), by applying a General
313 Time Reversible (GTR) model plus gamma-distributed rates and 4 substitution rate categories, a
314 fixed proportion of invariable sites, and a BioNJ starting tree (Guindon et al., 2009).
315 Differences in dN/dS among catarrhini-infecting SVs genes grouped on the basis of gene
316 conservation in the *Herpesvirales* order (Davison, 2007) were evaluated using the Wilcoxon rank
317 sum test.

318

319 **Detection of positive selection in the hominin-infecting simplexvirus lineage**

320 We analyzed a viral phylogeny composed of 53 catarrhini-infecting viral strains of *Simplexvirus*
321 genus. Specifically, we include 22 fully-sequenced strains infecting Old world monkey species (i.e.,
322 macaques and baboons), 1 strain infecting chimpanzee, and 30 strains infecting humans (both HSV-
323 1 and HSV-2, n=15 respectively). HSV-1 and HSV-2 strains were selected from clinical isolates with
324 no history of passaging in cell culture, sampled in different countries in order to have an
325 heterogeneous pool of viral genomes representative of the diversity among circulating strains
326 (Table S1).

327 Analyses were performed on the same phylogeny of catarrhini-infecting simplexviruses (see
328 above); for each coding-gene, phylogenetic trees were reconstructed using phyML. Each alignment
329 was screened for the presence of recombination using GARD (Kosakovsky Pond et al., 2006), a
330 genetic algorithm implemented in the HYPHY suite (version 2.2.4). When evidence of
331 recombination was detected (p value<0.01), the coding alignment was split accordingly; sub-
332 regions were then used as the input for molecular evolution analyses. Only resulting alignments
333 that, after GUIDANCE filtering had a length \geq 250 nt were considered for subsequent analyses.

334 Episodic positive selection on the Hominin-infecting simplexviruses branch was detected by
335 applying the branch-site likelihood ratio tests from codeml ("test 2") (Zhang et al., 2005). In this
336 test, a likelihood ratio test is applied to compare a model (MA) that allows positive selection on the
337 foreground lineages with a model (MA1) that does not allow such positive selection. Twice the
338 difference of likelihood for the two models ($\Delta\ln L$) is then compared to a χ^2 distribution with one
339 degree of freedom (Zhang et al., 2005). The analyses were performed using an F3X4 codon
340 frequency models. An FDR correction was applied to account for multiple tests.

341 To identify sites evolving under positive selection, we used BEB analysis from MA (with a cutoff of
342 0.90) and the Mixed Effects Model of Evolution (Murrell et al., 2012) (MEME, cutoff of 0.1), that
343 allows ω to vary from site to site and from branch to branch at a site. To limit false positives, only
344 sites confirmed by both methods were considered as positively selected.

345

346 **Plasmids**

347 The coding sequences of ICP47 N-terminus from HSV-1 (55aa, YP_009137148), HSV-2 (55aa,
348 YP_009137225.1), and B-virus (56aa, NP_851932) were synthesized and cloned in pCMV6-Entry
349 vector by Origene custom service. The pCMV6 vectors coding for the corresponding mutagenized
350 sequences were synthesized and cloned as well (Figure 4B).

351

352 **Cell culture and transfection**

353 Jurkat cells were cultured in RPMI complete media without antibiotics and supplemented with 10%
354 Fetal Bovine Serum (FBS). Cells were cultured at 37 °C and 5% CO₂ in Forma Steri-Cycle CO₂
355 incubator (Thermo). Every 3 days, cells were split to 0.5–1 × 10⁶ cells/ml in a T25 culture flask with
356 fresh media. ~5×10⁵ Jurkat cells were electroporated in a solution of R-buffer (100µL; Invitrogen)
357 containing 1ug of plasmid (HSV-1 full, N-term HSV-1, N-term HSV-1-mut N-term HSV-2, N-term
358 HSV-2 mut N-term B virus, N-term B virus mut) using a Neon® Transfection System (Invitrogen)
359 under the recommended electroporation condition (1350 V, 10 ms, 3 pulse). The transfected cells
360 were then seeded into 24-well plate. All experiments were run in four replicates and cells
361 electroporated without plasmid were considered as the control (mock).

362 Post transfection Jurkat cell viability was ≥90% as determined by an automatic cell counter (Digital
363 Bio, NanoEnTek Inc, Korea).

364

365 **Immunofluorescent staining and Flowcytometry analysis**

366 PBMCs were stained with HLA-ABC PE (Clone W6/32, eBioscience), and HLA-G PE-Cy7 (Isotype IgG2
367 Mouse, Clone 87G, eBioscience), for 15 min at room temperature in the dark. After incubation,
368 Jurkat cells were washed and resuspended in PBS.

369 Flow cytometric analyses were performed after 2 days post-transfection using a Beckman Coulter
370 Gallios Flow Cytometer equipped with two lasers operating at 488 and 638 nm, respectively,
371 interfaced with Gallios software and analyzed with Kaluza v 1.2. Two-hundred-thousand events
372 were acquired and gated on HLA-ABC or HLA-G for Jurkat cells.

373 Data were collected using linear amplifiers for forward and side scatter and logarithmic amplifiers
374 for fluorescence (FL)1, FL2, FL3, FL4, and FL5. Samples were first run using isotype control or single
375 fluorochrome-stained preparations for color compensation. Rainbow Calibration Particles
376 (Spherotec, Inc. Lake Forest, IL) were used to standardize flow-cytometry results.

377 Results were expressed as Mean Intensity Fluorescence (MFI) of HLA-ABC and HLA-G on Jurkat
378 cells.

379

380 **Funding**

381 This work was supported by the Italian Ministry of Health (“Ricerca Corrente 2019-2020” to MS,
382 “Ricerca Corrente 2018-2020” to DF)

383

384 **Competing interests**

385 The authors declare no conflict of interest

386

387 **References**

388

389 Arii, J., and Kawaguchi, Y. (2018). The Role of HSV Glycoproteins in Mediating Cell Entry. *Adv. Exp. Med. Biol.* **1045**, 3-21.10.1007/978-981-10-7230-7_1.

391 Arvin, A., Campadelli-Fiume, G., Mocarski, E., Moore, P.S., Roizman, B., Whitley, R., and Yamanishi,
392 K. (2007). *Human Herpesviruses. Biology, Therapy, and Immunoprophylaxis* (Cambridge: Cambridge
393 University Press).

394 Azab, W., Dayaram, A., Greenwood, A.D., and Osterrieder, N. (2018). How Host Specific Are
395 Herpesviruses? Lessons from Herpesviruses Infecting Wild and Endangered Mammals. *Annu. Rev. Virol.* **5**, 53-68.10.1146/annurev-virology-092917-043227.

397 Blondeau, C., Pelchen-Matthews, A., Mlcochova, P., Marsh, M., Milne, R.S., and Towers, G.J. (2013).
398 Tetherin restricts herpes simplex virus 1 and is antagonized by glycoprotein M. *J. Virol.* **87**, 13124-
399 13133.10.1128/JVI.02250-13.

400 Boyson, J.E., Iwanaga, K.K., Golos, T.G., and Watkins, D.I. (1997). Identification of a novel MHC class
401 I gene, Mamu-AG, expressed in the placenta of a primate with an inactivated G locus. *J. Immunol.*
402 **159**, 3311-3321.

403 Cairns, T.M., Fontana, J., Huang, Z.Y., Whitbeck, J.C., Atanasiu, D., Rao, S., Shelly, S.S., Lou, H., Ponce
404 de Leon, M., Steven, A.C., Eisenberg, R.J., and Cohen, G.H. (2014). Mechanism of neutralization of
405 herpes simplex virus by antibodies directed at the fusion domain of glycoprotein B. *J. Virol.* **88**,
406 2677-2689.10.1128/JVI.03200-13.

407 Chowdary, T.K., Cairns, T.M., Atanasiu, D., Cohen, G.H., Eisenberg, R.J., and Heldwein, E.E. (2010).
408 Crystal structure of the conserved herpesvirus fusion regulator complex gH-gL. *Nat. Struct. Mol.*
409 *Biol.* **17**, 882-888.10.1038/nsmb.1837.

410 Cooper, R.S., Georgieva, E.R., Borbat, P.P., Freed, J.H., and Heldwein, E.E. (2018). Structural basis for
411 membrane anchoring and fusion regulation of the herpes simplex virus fusogen gB. *Nat. Struct. Mol.*
412 *Biol.* **25**, 416-424.10.1038/s41594-018-0060-6.

413 Darling, A.C., Mau, B., Blattner, F.R., and Perna, N.T. (2004). Mauve: multiple alignment of
414 conserved genomic sequence with rearrangements. *Genome Res.* **14**, 1394-
415 1403.10.1101/gr.2289704.

416 Darling, A.E., Mau, B., and Perna, N.T. (2010). progressiveMauve: multiple genome alignment with
417 gene gain, loss and rearrangement. *PLoS One* *5*, e11147.10.1371/journal.pone.0011147.

418 Davison, A.J. (2007). Comparative analysis of the genomes. In *Human Herpesviruses: Biology,*
419 *Therapy, and Immunoprophylaxis*, Arvin, A., Campadelli-Fiume, G., Mocarski, E., Moore, P. S.,
420 Roizman, B., Whitley, R. and Yamanishi, K. eds., (Cambridge: Cambridge University Press), Chapter
421 2, pp. 10-26.

422 Deschamps, T., and Kalamvoki, M. (2017). Evasion of the STING DNA-Sensing Pathway by VP11/12
423 of Herpes Simplex Virus 1. *J. Virol.* *91*, e00535-17. doi: 10.1128/JVI.00535-17. Print 2017 Aug
424 15.10.1128/JVI.00535-17.

425 Deschaseaux, F., Delgado, D., Pistoia, V., Giuliani, M., Morandi, F., and Durrbach, A. (2011). HLA-G
426 in organ transplantation: towards clinical applications. *Cell Mol. Life Sci.* *68*, 397-
427 404.10.1007/s00018-010-0581-6.

428 Dubin, G., Socolof, E., Frank, I., and Friedman, H.M. (1991). Herpes simplex virus type 1 Fc receptor
429 protects infected cells from antibody-dependent cellular cytotoxicity. *J. Virol.* *65*, 7046-7050.

430 Dunn, W., Chou, C., Li, H., Hai, R., Patterson, D., Stolc, V., Zhu, H., and Liu, F. (2003). Functional
431 profiling of a human cytomegalovirus genome. *Proc. Natl. Acad. Sci. U. S. A.* *100*, 14223-
432 14228.10.1073/pnas.2334032100 .

433 Eberle, R., and Jones-Engel, L. (2018). Questioning the Extreme Neurovirulence of Monkey B Virus
434 (Macacine alphaherpesvirus 1). *Adv. Virol.* *2018*, 5248420.10.1155/2018/5248420.

435 Eberle, R., and Jones-Engel, L. (2017). Understanding Primate Herpesviruses. *J. Emerg. Dis. Virol.* *3*,
436 10.16966/2473-1846.127. Epub 2017 Jan 31.10.16966/2473-1846.127.

437 El Kasmi, I., and Lippé, R. (2015). Herpes simplex virus 1 gN partners with gM to modulate the viral
438 fusion machinery. *J. Virol.* *89*, 2313-2323.10.1128/JVI.03041-14.

439 Farooq, A.V., and Shukla, D. (2012). Herpes simplex epithelial and stromal keratitis: an
440 epidemiologic update. *Surv. Ophthalmol.* *57*, 448-462.10.1016/j.survophthal.2012.01.005.

441 Forni, D., Cagliani, R., Tresoldi, C., Pozzoli, U., De Gioia, L., Filippi, G., Riva, S., Menozzi, G., Colleoni,
442 M., Biasin, M., Lo Caputo, S., Mazzotta, F., Comi, G.P., Bresolin, N., Clerici, M., and Sironi, M. (2014).
443 An Evolutionary Analysis of Antigen Processing and Presentation across Different Timescales
444 Reveals Pervasive Selection. *PLoS Genet.* *10*, e1004189.10.1371/journal.pgen.1004189;
445 10.1371/journal.pgen.1004189.

446 Früh, K., Ahn, K., Djaballah, H., Sempé, P., van Endert, P.M., Tampé, R., Peterson, P.A., and Yang, Y.
447 (1995). A viral inhibitor of peptide transporters for antigen presentation. *Nature* 375, 415-
448 418.10.1038/375415a0.

449 Galocha, B., Hill, A., Barnett, B.C., Dolan, A., Raimondi, A., Cook, R.F., Brunner, J., McGeoch, D.J.,
450 and Ploegh, H.L. (1997). The active site of ICP47, a herpes simplex virus-encoded inhibitor of the
451 major histocompatibility complex (MHC)-encoded peptide transporter associated with antigen
452 processing (TAP), maps to the NH₂-terminal 35 residues. *J. Exp. Med.* 185, 1565-
453 1572.10.1084/jem.185.9.1565.

454 Gianni, T., Leoni, V., Chesnokova, L.S., Hutt-Fletcher, L.M., and Campadelli-Fiume, G. (2012). α V β 3-
455 Integrin is a Major Sensor and Activator of Innate Immunity to Herpes Simplex Virus-1. *Proc. Natl.*
456 *Acad. Sci. U. S. A.* 109, 19792-19797.10.1073/pnas.1212597109.

457 Gilardi, K.V., Oxford, K.L., Gardner-Roberts, D., Kinani, J.F., Spelman, L., Barry, P.A., Cranfield, M.R.,
458 and Lowenstine, L.J. (2014). Human herpes simplex virus type 1 in confiscated gorilla. *Emerg.*
459 *Infect. Dis.* 20, 1883-1886.10.3201/eid2011.140075.

460 Guindon, S., Delsuc, F., Dufayard, J.F., and Gascuel, O. (2009). Estimating maximum likelihood
461 phylogenies with PhyML. *Methods Mol. Biol.* 537, 113-137.10.1007/978-1-59745-251-9_6;
462 10.1007/978-1-59745-251-9_6.

463 Gupta, R.K., Hué, S., Schaller, T., Verschoor, E., Pillay, D., and Towers, G.J. (2009). Mutation of a
464 single residue renders human tetherin resistant to HIV-1 Vpu-mediated depletion. *PLoS Pathog.* 5,
465 e1000443.10.1371/journal.ppat.1000443.

466 Heldwein, E.E., Lou, H., Bender, F.C., Cohen, G.H., Eisenberg, R.J., and Harrison, S.C. (2006). Crystal
467 structure of glycoprotein B from herpes simplex virus 1. *Science* 313, 217-220.313/5784/217.

468 Hill, A., Jugovic, P., York, I., Russ, G., Bennink, J., Yewdell, J., Ploegh, H., and Johnson, D. (1995).
469 Herpes simplex virus turns off the TAP to evade host immunity. *Nature* 375, 411-
470 415.10.1038/375411a0.

471 Huard, B., and Früh, K. (2000). A role for MHC class I down-regulation in NK cell lysis of herpes
472 virus-infected cells. *Eur. J. Immunol.* 30, 509-515. 10.1002/1521-4141(200002)30:2<509::AID-
473 IMMU509>3.0.CO;2-H.

474 Katoh, K., and Standley, D.M. (2013). MAFFT multiple sequence alignment software version 7:
475 improvements in performance and usability. *Mol. Biol. Evol.* *30*, 772-780.10.1093/molbev/mst010;
476 10.1093/molbev/mst010.

477 Kosakovsky Pond, S.L., and Frost, S.D. (2005). Not so different after all: a comparison of methods
478 for detecting amino acid sites under selection. *Mol. Biol. Evol.* *22*, 1208-1222.msi105.

479 Kosakovsky Pond, S.L., Posada, D., Gravenor, M.B., Woelk, C.H., and Frost, S.D. (2006). Automated
480 phylogenetic detection of recombination using a genetic algorithm. *Mol. Biol. Evol.* *23*, 1891-
481 1901.10.1093/molbev/msl051.

482 Lee, N., Malacko, A.R., Ishitani, A., Chen, M.C., Bajorath, J., Marquardt, H., and Geraghty, D.E.
483 (1995). The membrane-bound and soluble forms of HLA-G bind identical sets of endogenous
484 peptides but differ with respect to TAP association. *Immunity* *3*, 591-600.1074-7613(95)90130-2.

485 Leoni, V., Gianni, T., Salvioli, S., and Campadelli-Fiume, G. (2012). Herpes simplex virus
486 glycoproteins gH/gL and gB bind Toll-like receptor 2, and soluble gH/gL is sufficient to activate NF-
487 κB. *J. Virol.* *86*, 6555-6562.10.1128/JVI.00295-12.

488 Lim, E.S., Malik, H.S., and Emerman, M. (2010). Ancient adaptive evolution of tetherin shaped the
489 functions of Vpu and Nef in human immunodeficiency virus and primate lentiviruses. *J. Virol.* *84*,
490 7124-7134.10.1128/JVI.00468-10.

491 Liu, Y., Luo, S., He, S., Zhang, M., Wang, P., Li, C., Huang, W., Hu, B., Griffin, G.E., Shattock, R.J., and
492 Hu, Q. (2015). Tetherin restricts HSV-2 release and is counteracted by multiple viral glycoproteins.
493 *Virology* *475*, 96-109.50042-6822(14)00499-1.

494 Looker, K.J., Magaret, A.S., May, M.T., Turner, K.M., Vickerman, P., Gottlieb, S.L., and Newman, L.M.
495 (2015a). Global and Regional Estimates of Prevalent and Incident Herpes Simplex Virus Type 1
496 Infections in 2012. *PLoS One* *10*, e0140765.10.1371/journal.pone.0140765.

497 Looker, K.J., Magaret, A.S., Turner, K.M., Vickerman, P., Gottlieb, S.L., and Newman, L.M. (2015b).
498 Global estimates of prevalent and incident herpes simplex virus type 2 infections in 2012. *PLoS One*
499 *10*, e114989.10.1371/journal.pone.0114989.

500 Loomis, M.R., O'Neill, T., Bush, M., and Montali, R.J. (1981). Fatal herpesvirus infection in patas
501 monkeys and a black and white colobus monkey. *J. Am. Vet. Med. Assoc.* *179*, 1236-1239.

502 Malito, E., Chandramouli, S., and Carfi, A. (2018). From recognition to execution-the HCMV
503 Pentamer from receptor binding to fusion triggering. *Curr. Opin. Virol.* 31, 43-51.S1879-
504 6257(18)30015-4.

505 Matschulla, T., Berry, R., Gerke, C., Döring, M., Busch, J., Paijo, J., Kalinke, U., Momburg, F., Hengel,
506 H., and Halenius, A. (2017). A highly conserved sequence of the viral TAP inhibitor ICP47 is required
507 for freezing of the peptide transport cycle. *Sci. Rep.* 7, 2933-017-02994-5.10.1038/s41598-017-
508 02994-5.

509 Matundan, H., and Ghiasi, H. (2019). Herpes Simplex Virus 1 ICP22 Suppresses CD80 Expression by
510 Murine Dendritic Cells. *J. Virol.* 93, e01803-18. doi: 10.1128/JVI.01803-18. Print 2019 Feb
511 1.10.1128/JVI.01803-18.

512 McGeoch, D.J., Rixon, F.J., and Davison, A.J. (2006). Topics in herpesvirus genomics and evolution.
513 *Virus Res.* 117, 90-104.S0168-1702(06)00021-9.

514 McNatt, M.W., Zang, T., Hatziloannou, T., Bartlett, M., Fofana, I.B., Johnson, W.E., Neil, S.J., and
515 Bieniasz, P.D. (2009). Species-specific activity of HIV-1 Vpu and positive selection of tetherin
516 transmembrane domain variants. *PLoS Pathog.* 5, e1000300.10.1371/journal.ppat.1000300.

517 Morandi, F., Rizzo, R., Fainardi, E., Rouas-Freiss, N., and Pistoia, V. (2016). Recent Advances in Our
518 Understanding of HLA-G Biology: Lessons from a Wide Spectrum of Human Diseases. *J. Immunol.*
519 *Res.* 2016, 4326495.10.1155/2016/4326495.

520 Mozzi, A., Biolatti, M., Cagliani, R., Forni, D., Dell'Oste, V., Pontremoli, C., Vantaggiato, C., Pozzoli,
521 U., Clerici, M., Landolfo, S., and Sironi, M. (2020). Past and ongoing adaptation of human
522 cytomegalovirus to its host. *PLoS Pathog.* 16, e1008476.10.1371/journal.ppat.1008476.

523 Mozzi, A., Pontremoli, C., Forni, D., Clerici, M., Pozzoli, U., Bresolin, N., Cagliani, R., and Sironi, M.
524 (2015). OASes and STING: adaptive evolution in concert. *Genome Biol. Evol.* 7, 1016-
525 1032.10.1093/gbe/evv046.

526 Murrell, B., Wertheim, J.O., Moola, S., Weighill, T., Scheffler, K., and Kosakovsky Pond, S.L. (2012).
527 Detecting individual sites subject to episodic diversifying selection. *PLoS Genet.* 8,
528 e1002764.10.1371/journal.pgen.1002764.

529 Oldham, M.L., Grigorieff, N., and Chen, J. (2016). Structure of the transporter associated with
530 antigen processing trapped by herpes simplex virus. *eLife* 5, 10.7554/eLife.21829.e21829 [pii]

531 Orange, J.S. (2013). Natural killer cell deficiency. *J. Allergy Clin. Immunol.* **132**, 515-525.S0091-
532 6749(13)01123-8.

533 Privman, E., Penn, O., and Pupko, T. (2012). Improving the performance of positive selection
534 inference by filtering unreliable alignment regions. *Mol. Biol. Evol.* **29**, 1-
535 5.10.1093/molbev/msr177.

536 Rager-Zisman, B., Quan, P.C., Rosner, M., Moller, J.R., and Bloom, B.R. (1987). Role of NK cells in
537 protection of mice against herpes simplex virus-1 infection. *J. Immunol.* **138**, 884-888.

538 Rothenburg, S., and Brennan, G. (2020). Species-Specific Host-Virus Interactions: Implications for
539 Viral Host Range and Virulence. *Trends Microbiol.* **28**, 46-56.S0966-842X(19)30220-3.

540 Sela, I., Ashkenazy, H., Katoh, K., and Pupko, T. (2015). GUIDANCE2: accurate detection of
541 unreliable alignment regions accounting for the uncertainty of multiple parameters. *Nucleic Acids
542 Res.* **43**, W7-14.10.1093/nar/gkv318.

543 Severini, A., Tyler, S.D., Peters, G.A., Black, D., and Eberle, R. (2013). Genome sequence of a
544 chimpanzee herpesvirus and its relation to other primate alphaherpesviruses. *Arch. Virol.* **158**,
545 1825-1828.10.1007/s00705-013-1666-y.

546 Sironi, M., Cagliani, R., Forni, D., and Clerici, M. (2015). Evolutionary insights into host-pathogen
547 interactions from mammalian sequence data. *Nat. Rev. Genet.* **16**, 224-236.10.1038/nrg3905.

548 Slukvin, I.I., Lunn, D.P., Watkins, D.I., and Golos, T.G. (2000). Placental expression of the nonclassical
549 MHC class I molecule Mamu-AG at implantation in the rhesus monkey. *Proc. Natl. Acad. Sci. U. S. A.*
550 97, 9104-9109.97/16/9104.

551 Sprague, E.R., Wang, C., Baker, D., and Bjorkman, P.J. (2006). Crystal structure of the HSV-1 Fc
552 receptor bound to Fc reveals a mechanism for antibody bipolar bridging. *PLoS Biol.* **4**, e148.e148.

553 Striebinger, H., Funk, C., Raschbichler, V., and Bailer, S.M. (2016). Subcellular Trafficking and
554 Functional Relationship of the HSV-1 Glycoproteins N and M. *Viruses* **8**, 83.10.3390/v8030083.

555 Temme, S., Eis-Hübinger, A.M., McLellan, A.D., and Koch, N. (2010). The herpes simplex virus-1
556 encoded glycoprotein B diverts HLA-DR into the exosome pathway. *J. Immunol.* **184**, 236-
557 243.10.4049/jimmunol.0902192.

558 Tischer, B.K., and Osterrieder, N. (2010). Herpesviruses--a zoonotic threat? *Vet. Microbiol.* **140**,
559 266-270.10.1016/j.vetmic.2009.06.020.

560 Tognarelli, E.I., Palomino, T.F., Corrales, N., Bueno, S.M., Kalergis, A.M., and González, P.A. (2019).
561 Herpes Simplex Virus Evasion of Early Host Antiviral Responses. *Front. Cell. Infect. Microbiol.* 9,
562 127.10.3389/fcimb.2019.00127.

563 Tomazin, R., van Schoot, N.E., Goldsmith, K., Jugovic, P., Sempé, P., Früh, K., and Johnson, D.C.
564 (1998). Herpes simplex virus type 2 ICP47 inhibits human TAP but not mouse TAP. *J. Virol.* 72, 2560-
565 2563.1747.

566 Trgovcich, J., Johnson, D., and Roizman, B. (2002). Cell surface major histocompatibility complex
567 class II proteins are regulated by the products of the gamma(1)34.5 and U(L)41 genes of herpes
568 simplex virus 1. *J. Virol.* 76, 6974-6986.0163.

569 Underdown, S.J., Kumar, K., and Houldcroft, C. (2017). Network analysis of the hominin origin of
570 Herpes Simplex virus 2 from fossil data. *Virus Evol.* 3, vex026.10.1093/ve/vex026.

571 van de Weijer, M.L., Luteijn, R.D., and Wiertz, E.J. (2015). Viral immune evasion: Lessons in MHC
572 class I antigen presentation. *Semin. Immunol.* 27, 125-137.S1044-5323(15)00018-4.

573 Vasireddi, M., and Hilliard, J. (2012). Herpes B virus, macacine herpesvirus 1, breaks simplex virus
574 tradition via major histocompatibility complex class I expression in cells from human and macaque
575 hosts. *J. Virol.* 86, 12503-12511.10.1128/JVI.01350-12.

576 Verweij, M.C., Horst, D., Griffin, B.D., Luteijn, R.D., Davison, A.J., Ressing, M.E., and Wiertz, E.J.
577 (2015). Viral inhibition of the transporter associated with antigen processing (TAP): a striking
578 example of functional convergent evolution. *PLoS Pathog.* 11,
579 e1004743.10.1371/journal.ppat.1004743.

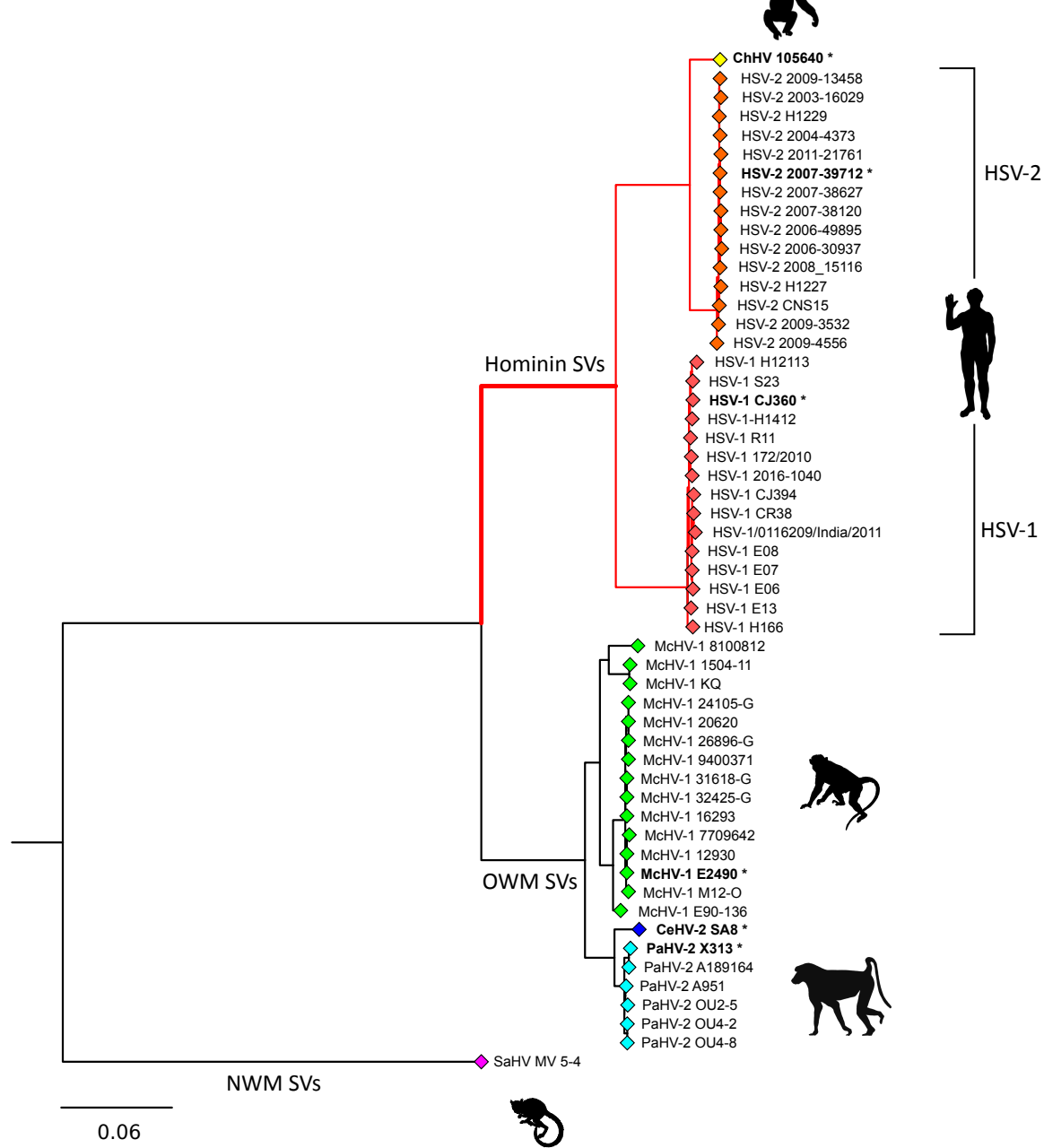
580 Wertheim, J.O., Smith, M.D., Smith, D.M., Scheffler, K., and Kosakovsky Pond, S.L. (2014).
581 Evolutionary origins of human herpes simplex viruses 1 and 2. *Mol. Biol. Evol.* 31, 2356-
582 2364.10.1093/molbev/msu185.

583 Whitley, R. (2004). Neonatal herpes simplex virus infection. *Curr. Opin. Infect. Dis.* 17, 243-
584 246.00001432-200406000-00012 .

585 Wilson, R.B., Holscher, M.A., Chang, T., and Hodges, J.R. (1990). Fatal Herpesvirus simiae (B virus)
586 infection in a patas monkey (*Erythrocebus patas*). *J. Vet. Diagn. Invest.* 2, 242-
587 244.10.1177/104063879000200321.

588 Zhang, J., Nielsen, R., and Yang, Z. (2005). Evaluation of an improved branch-site likelihood method
589 for detecting positive selection at the molecular level. *Mol. Biol. Evol.* 22, 2472-
590 2479.10.1093/molbev/msi237.

A



B

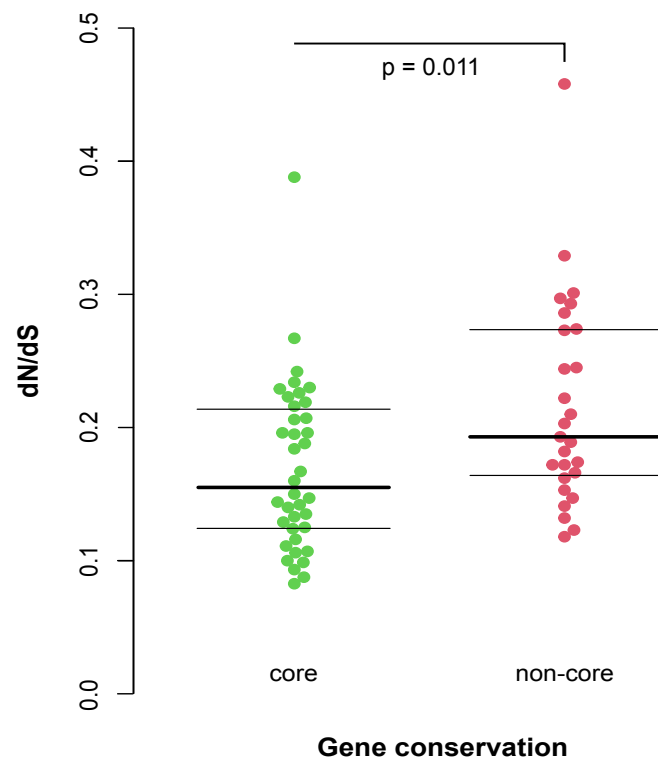
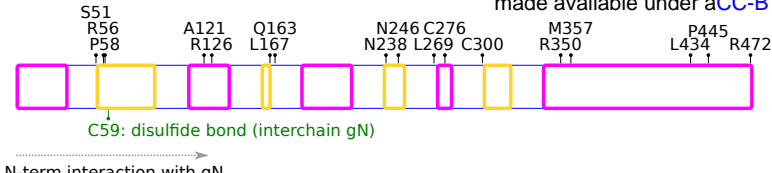


Figure 1. Selective patterns of primate simplexviruses.

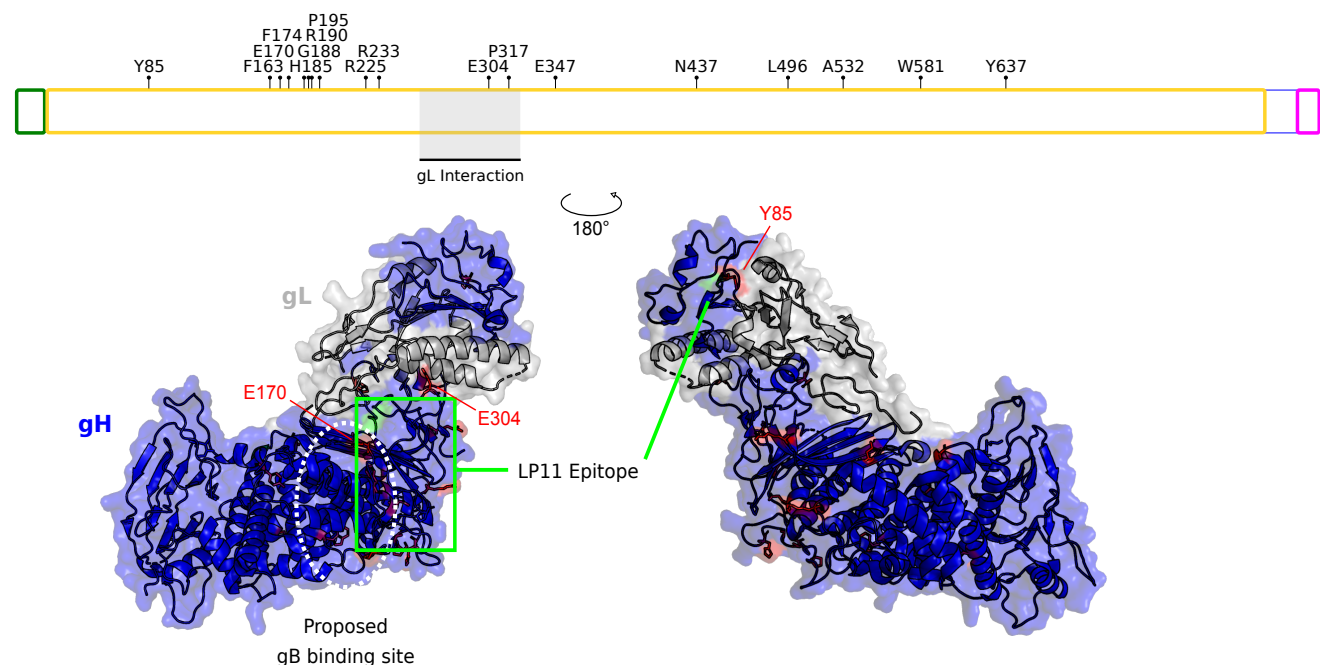
(A) A maximum-likelihood tree of glycoprotein B (encoded by the UL27 core gene) is drawn to exemplify the phylogenetic relationships among primate simplexviruses (Strain information and GeneBank IDs are reported in Table S1). The *Saimiriine alphaherpesvirus 1* (GeneBank ID: NC_014567) was used as the outgroup and the tree was constructed using PhyML (see methods). Asterisks denote viruses that were included in the analysis of selective patterns of catarrhini-infecting SVs. The hominin simplexvirus branch, that was specifically tested for episodic positive selection, is shown in red. (B) Comparison of dN/dS between *core* and *non-core* genes. The p value was calculated by the Wilcoxon Rank-Sum test.

LEGEND:

- Signal peptide
- Surface exposed
- Intravirion or intracellular
- Transmembrane region
- Other, mixed or unknown



UL22 - Envelope glycoprotein H



UL27 - Envelope glycoprotein B

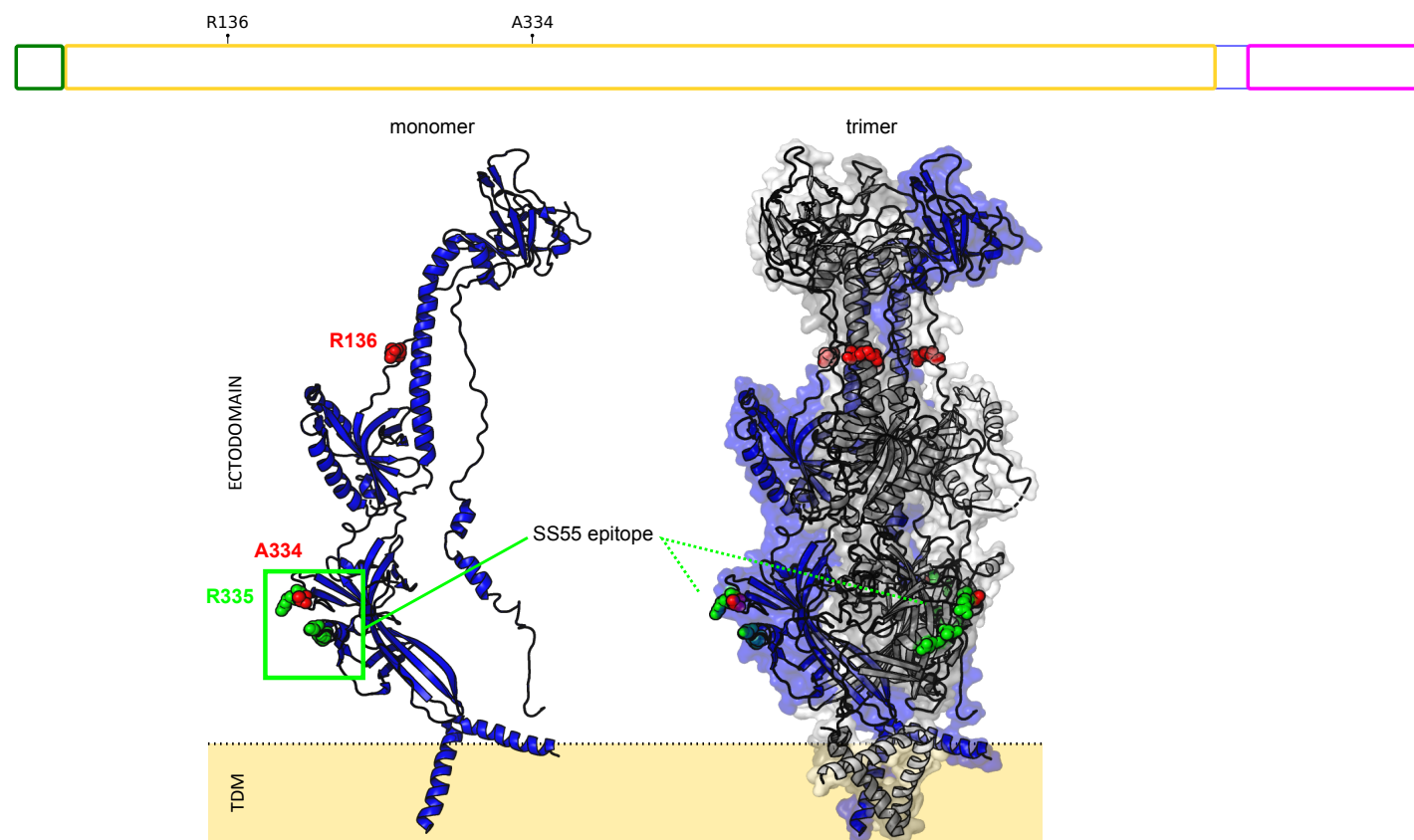
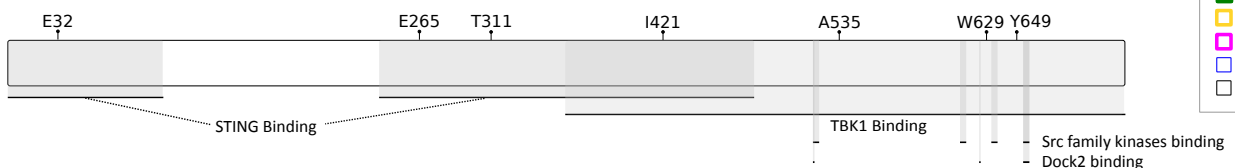


Figure 2. Positive selection in simplexvirus glycoproteins. Positively selected sites were mapped onto HSV-1 glycoproteins together with the location of functional domain/sites (grey). Topological features are color-coded according to the legend. For gH, positively selected sites (red) were mapped onto the three-dimensional structure of the gH-gL complex (blue and white, respectively; PDB ID: 3m1c) (Chowdary et al., 2010). The location of the LP11 epitope (green) and of the gB binding sites (white) are reported. The two views are rotated 180° around the vertical axis. For gB, positively selected sites were mapped onto the three-dimensional structures of the gB monomer (PDB ID: 6bm8) (Cooper et al., 2018) and the trimeric gB complex. This latter was obtained by a structural imposition of the monomer, using the 2gum structure as scaffold (Heldwein et al., 2006). The location of the SS55 epitope is reported in green. Positions refer to the reference HSV-1 strain 17 (NC_001806).

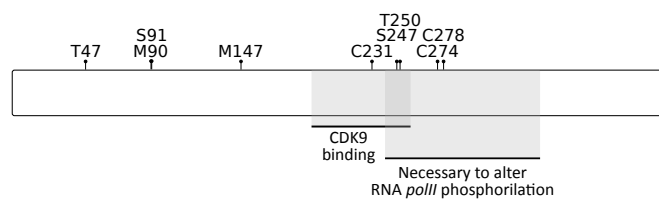
LEGEND

- █ Signal peptide
- █ Surface exposed
- █ Intravirion/intracellular
- █ Transmembrane region
- █ Other, mixed or unknown

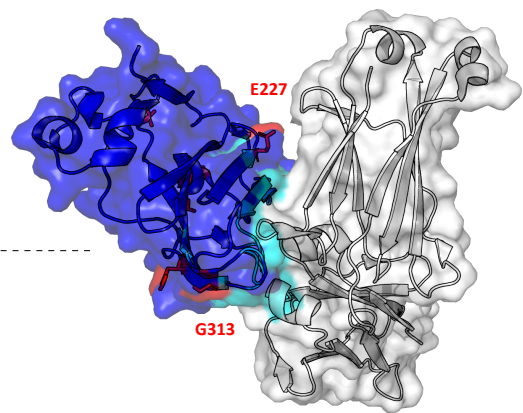
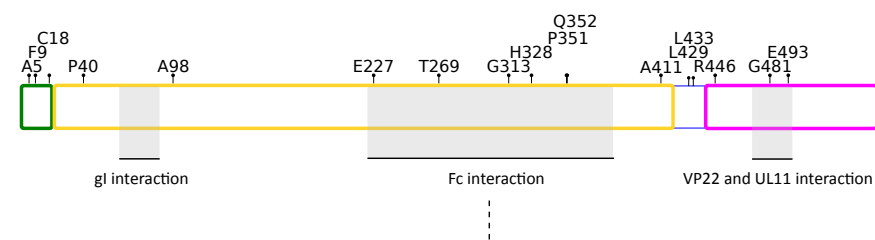
UL46 - Tegument protein VP11/12



US1 - Regulatory protein ICP22



US8 - Envelope glycoprotein E



US12 - TAP transporter inhibitor ICP47

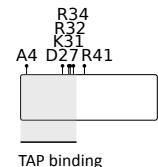


Figure 3. Positive selection in SVs proteins involved in host immune system-escape. Proteins and positively selected sites are reported as in Figure 2. For gE, the three-dimensional structure of the complex with Fc (PDB ID:2gj7) is reported (Sprague et al., 2006). gE is represented in blue, with the Fc interaction surface in cyan. Positively selected sites are in red. Positions refer to the reference HSV-1 strain 17 (NC_001806).

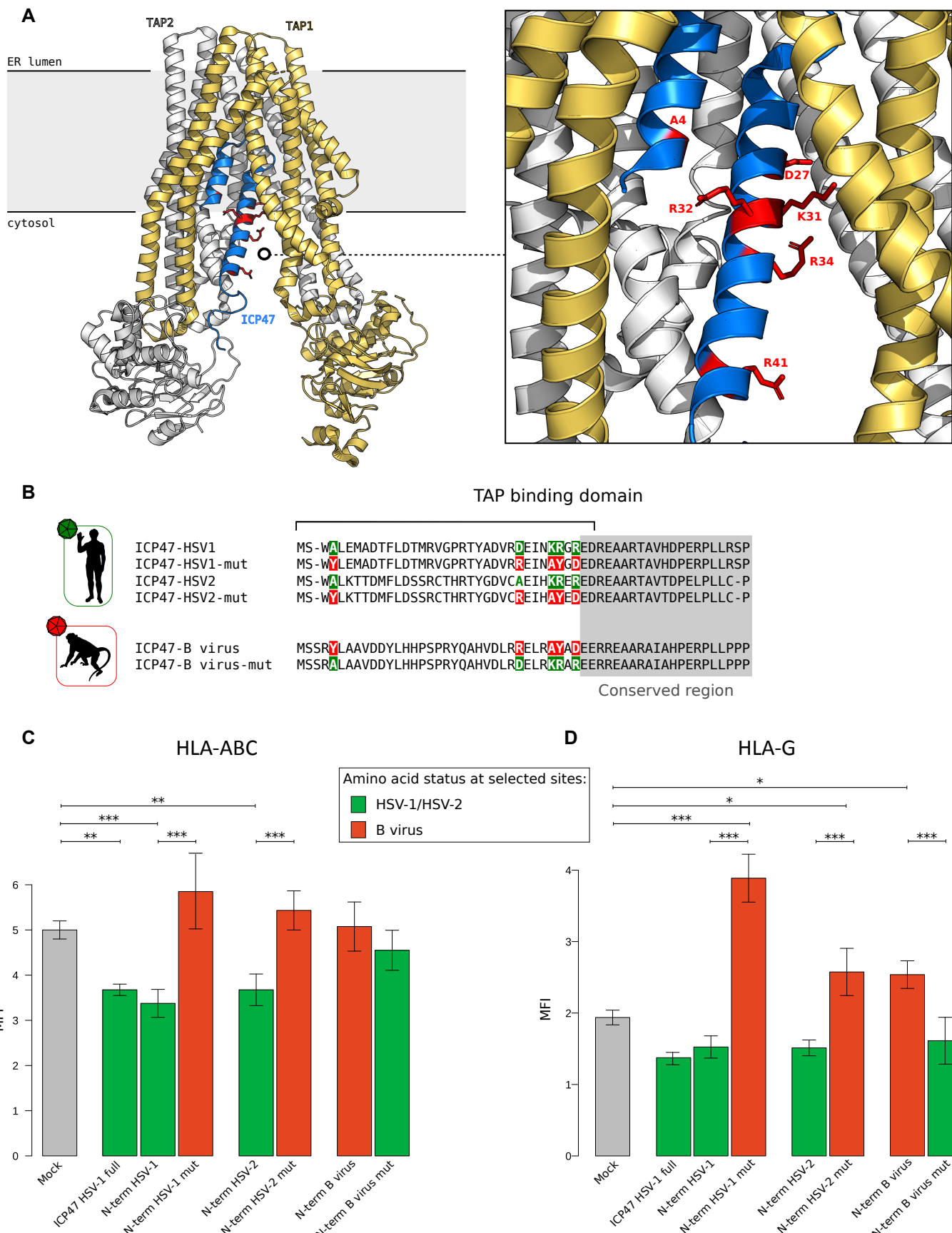


Figure 4. Functional characterization of positive selected sites of US12 (ICP47). (A) Ribbon representation of the three-dimensional structure of ICP47 bound to the TAP transporter, which in turn is composed by two subunits, TAP1 (light orange) and TAP2 (white) (PDB ID: 5u1d) (Oldham et al., 2016). Positively selected sites are represented as red sticks in the enlargement. (B) Schematic view recapitulating the amino state of positively selected sites tested in our analyses.

HLA-ABC (C) and HLA-G (D) expression at the cell surface. Jurkat cells were transfected with the ICP47 constructs and the amounts of total HLA-ABC or HLA-G antigen was quantified by cytofluorimetry after 48 hours. MFI (mean fluorescence intensity) bar plots represent the mean and standard deviation of four replicates. *p* values were calculated using Tukey post hoc tests.